bond, indicated by the comparatively downfield shift ($\delta =$ 8.11) of the amide N–H resonance was unambiguously demonstrated by comparison of the amide N–H shifts in the spectra (in $CDCl_3$) of the carbamate **8** and the amine **9** when the signal of the amide N–H appeared significantly shifted upfield ($\Delta\delta = 1.61$) after removal of the Boc unit. Besides the main conformational population, VT NMR experiments which showed a significant chemical-shift change ($\Delta\delta/\Delta T = -5.2\ \mathrm{ppb\,K^{-1}}$) gave evidence for a temperature dependant coexistence of non-hydrogen bonded conformations,[17] corroborated by NOEs between H-3 and the carbamate N-H at elevated temperature (330 K, $CDCl_3$). The FT-infrared (IR) spectrum displayed an extensive absorption at 3350 cm^{-1} characteristic for a hydrogen bonded amide and an absorption at 3405 cm^{-1} also indicating the coexistence of a solvent-exposed amide.

In conclusion, a highly efficient proline-based type VI β-turn mimetic was designed employing the results of molecular dynamics simulation. EPC synthesis involving Seebach's self-reproduction of chirality methodology and Grubbs' ring-closing olefin metathesis gave access to the novel molecular scaffold.

Received: March 12, 2001
Revised: June 26, 2001 [Z16752]

[1] M. S. P. Sansom, H. Weinstein, *Trends Pharmacol. Sci.* **2000**, *21*, 445–451.
[2] S. Fischer, R. L. Dunbrack, Jr., M. Karplus, *J. Am. Chem. Soc.* **1994**, *116*, 11931–11937.
[3] A. Wittelsberger, M. Keller, L. Scarpellino, L. Patiny, H. Acha-Orbea, M. Mutter, *Angew. Chem.* **2000**, *112*, 1153–1156; *Angew. Chem. Int. Ed.* **2000**, *39*, 1111–1115.
[4] D. Gramberg, C. Weber, R. Beeli, J. Inglis, C. Bruns, J. A. Robinson, *Helv. Chim. Acta* **1995**, *78*, 1588–1606.
[5] K. Kim, J. P. Germanas, *J. Org. Chem.* **1997**, *62*, 2847–2852.
[6] G. Müller, G. Hessler, H. Y. Decornez, *Angew. Chem.* **2000**, *112*, 926–928; *Angew. Chem. Int. Ed.* **2000**, *39*, 894–896.
[7] D. Seebach, M. Boes, R. Naef, W. B. Schweizer, *J. Am.Chem. Soc.* **1983**, *105*, 5390–5398.
[8] a) R. H. Grubbs, S. Chang, *Tetrahedron* **1998**, *54*, 4413–4450; b) M. Schuster, S. Blechert, *Angew. Chem.* **1997**, *109*, 2124–2144; *Angew. Chem. Int. Ed. Engl.* **1997**, *36*, 2036–2055; c) A. Fürstner, *Angew. Chem.* **2000**, *112*, 3140–3172; *Angew. Chem. Int. Ed.* **2000**, *39*, 3012–3043.
[9] H. Wang, J. P. Germanas, *Synlett* **1999**, *7*, 33–36.
[10] P. Schwab, R. H. Grubbs, J. W. Ziller, *J. Am. Chem. Soc.* **1996**, *118*, 100–110.
[11] a) "Alkene Metathesis in Organic Synthesis": A. Fürstner, *Top. Organomet. Chem.* **1998**, *1*, 37–72; b) E. L. Dias, S. T. Nguyen, R. H. Grubbs, *J. Am. Chem. Soc.* **1997**, *118*, 3887–3897.
[12] M. Ulman, R. H. Grubbs, *J. Org. Chem.* **1999**, *64*, 7202–7207.
[13] T. Clark, A. Alex, B. Beck, J. Chandrasekar, P. Gedeck, A. Horn, M. Hutter, B. Martin, G. Rauhut, W. Sauer, T. Schindler, T. Steinke, *Programme Package VAMP 7.0*, Oxford Molecular Group Plc., Oxford, **1998**.
[14] J. A. Robinson, *Synlett* **2000**, *4*, 429–441.
[15] A. Klamt, G. Schüürmann, *J. Chem. Soc. Perkin Trans. 2* **1993**, 799–805.
[16] M. Scholl, S. Ding, C. W. Lee, R. H. Grubbs, *Org. Lett.* **1999**, *1*, 953–956.
[17] a) L. Belvisi, C. Gennari, A. Mielgo, D. Potenza, C. Scolastico, *Eur. J. Org. Chem.* **1999**, 389–400; b) E. S. Stevens, N. Sugawara, C. M. Bonora, C. Toniolo, *J. Am. Chem. Soc.* **1980**, *102*, 7048–7050; c) K. Weber, U. Ohnmacht, P. Gmeiner, *J. Org. Chem.* **2000**, *65*, 7406–7416.

Atomic Force Microscope Studies on Condensation of Plasmid DNA with Functionalized Fullerenes**

Hiroyuki Isobe, Sho Sugiyama, Ken-ichi Fukui, Yasuhiro Iwasawa, and Eiichi Nakamura*

A recent paper reported the first example of the use of a carbon cluster as a vector to deliver DNA into mammalian cells.[1, 2] Thus, mixed with the tailor-made tetraminofullerene **1**, a plasmid DNA forms micrometer-sized fullerene–DNA particles as observed by optical microscope, which, after

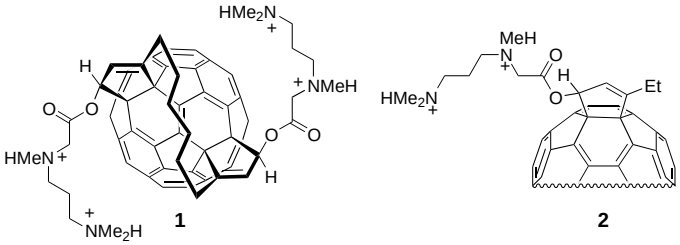

1 **2**

incubation with the target cells, became located inside the cytoplasm as phagocytes. Expression of the encoded gene took place over several days, indicating that the plasmid DNA was released into the cytoplasm without being damaged by the fullerene complexation. Although these biological experiments demonstrated the ability of the fullerene **1** to condense and release DNA, the molecular nature of such reversible DNA condensation remained unclear. We report herein the results of atomic force microscope (AFM) studies[3] that provided molecular-level information on the DNA condensation/release processes induced by fullerene vesicles.[4] When used in a small quantity, the fullerene **1** condenses a single plasmid DNA into a **1**–DNA complex. Upon further addition of **1**, many single-molecule DNA condensates gather together to form the micrometer-sized fullerene–DNA particles observed previously by optical microscopy. Release of the DNA molecules from these large particles was achieved experimentally by removal of the fullerene through $CHCl_3$ extraction.

The interactions between the fullerene **1** and DNA were probed for 4 kbp supercoiled plasmid DNA (pBR322). Thus, we added an increasing amount of **1** to a pH 7.6 buffer solution of pBR322 and plotted the amount of the DNA mobile on the gel against the reagent/base pair ratio (R). As shown in Figure 1 (solid line), there was observed precipitous decrease

[*] Prof. Dr. E. Nakamura, Dr. H. Isobe, S. Sugiyama, Dr. K.-i. Fukui, Prof. Dr. Y. Iwasawa
Department of Chemistry
The University of Tokyo
Hongo, Bunkyo-ku, Tokyo 113-0033 (Japan)
Fax: (+81) 3-5800-6889
E-mail: nakamura@chem.s.u-tokyo.ac.jp

[**] This research was supported by Grant-in-Aid for Specially Promoted Research from Ministry of Education, Culture, Sports, Science, and Technology.

Supporting information for this article is available on the WWW under http://www.angewandte.com or from the author.

  1433-7851/01/4018-3364 $ 17.50+.50/0

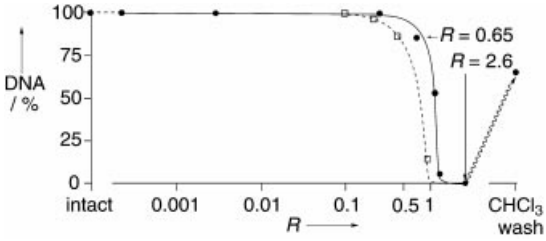

Figure 1. Amount of pBR322 plasmid DNA remaining in solution as determined by gel electrophoresis (integrated optical density of fluorescence, solid line) and by CD spectra (molar ellipticity spectra at 260 nm, broken line) in the presence of **1** at various R values. The y-axis (DNA) is relative to the value obtained for $R = 0$.

of the DNA mobile on the gel for R values between 0.5 and 1.8. With this latter ratio, no mobile DNA was detected on the gel. Note that $R = 0.5$ is the theoretical point of neutralization of the DNA phosphate charges with the tetraminofullerene **1** at pH 7. Although no further change was observed upon addition (and removal) of EtOH (in which **1** does not dissolve), we found that extraction of the mixture with $CHCl_3$ results in the reappearance of about 70% of the supercoiled DNA on the gel. No DNA nicking was observed in the recovered DNA. Since $CHCl_3$ freely dissolves the fullerene **1**, we conclude that DNA was released from the fullerene–DNA precipitate as the fullerene was washed away. Thus, the fullerene–DNA binding is not covalent. Note that the one-handed analog **2**, which binds to DNA very weakly,[1] did not cause DNA precipitation even at $R = 2.6$.[5]

Measurement of the CD spectra of the fullerene–DNA mixture (Figure 2) afforded further information on the complexation process. Thus, the molar ellipticity $[\theta]$ at 260 nm starts to decrease at $R \sim 0.4$ and becomes nearly zero

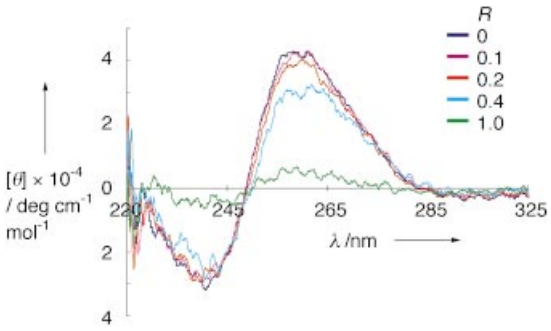

Figure 2. CD spectra of plasmid pBR322 DNA in the presence of **1** at R values between 0–1. CD spectra were measured in a THF/Mg-HEPES buffer (20% v/v, [bp] = 100 μM, pH 7.6). See Supporting Information for details of the experimental procedure.

at $R = 1.0$ (namely, loss of the DNA from solution). The $[\theta]/R$ plot (broken line) in Figure 1 is parallel to the result of the gel experiment. The systematic difference between the two lines can be ascribed to the electric field applied in the gel electrophoresis, which will strip the positively charged fullerene and the negatively charged DNA off from the fullerene–DNA complex, thereby increasing the amount of mobile DNA on the gel. More importantly, the plasmid DNA in the soluble fraction, for which the AFM images in Figures 3c and 4d were obtained, exhibited CD spectra characteristic of a B-helix (Figure 2).

Whereas the above experiments revealed only one phase transition event for the R range between 2.5×10^{-4} and 2.6, AFM analysis of the same mixture revealed that more complex events are taking place in the fullerene complexation process (Figures 3 and 4). Upon dissolution in the buffer solution, the fullerene **1** forms vesicles, which were observed as numerous humps in a thin aqueous films on mica surface (Figure 3a) as recently reported for an analogous water-soluble fullerene.[4a] Each vesicle may contains several thousand fullerene molecules.[4b] The solution of the intact DNA used for the gel experiments revealed a large number of overlapping molecules (Figure 3b), and a highly diluted solution of the same DNA showed separated molecules (Figure 4a).

A noteworthy AFM observation was made in the analysis of the soluble fraction at $R = 0.65$ (Figure 3c), where neither gel nor CD data suggested any change of the DNA structure. When the mixture was spotted on a mica surface, the surface was covered by numerous flat disks of rather narrow size distribution. The smallest disks, which were the most abundant, measured about 50 nm in diameter and 3 nm in thickness with a calculated volume of 5×10^3 nm^3, which is only 25% larger than the volume of pBR322 DNA (4×10^3 nm^3 when approximated as a rod). Unlike the fullerene vesicles, which are soft and dome-shaped (Figure 3a and ref. [4a]), the disks are rather flat and their top surface shows a fine structure (Figure 4d). Beside the small disks, we also found larger disks, which have the same thickness but are two or three times larger in diameter than the smallest disks. Though the large area of the mica surface was covered by the disks, we found in some areas partially folded objects (Figures 3d, 4b, and 4c).[6] In Figures 4b and 4c, we can identify intact double strands between the partially condensed parts. Taken together with the volume and shape analysis of the disks (see below), comparison of these objects (Figures 4b and 4c) with the intact DNA (Figure 4a) and the disks (Figure 4d) strongly suggest that the smallest disk is a single DNA molecule condensed through interaction with the fullerene. We therefore formulate the DNA folding process as the sequence of Figures 4a → 4b → 4c → 4d. Likewise, we consider that the double- and triple-sized disks of are two- and three-molecular condensates. The shape and the size distribution of the fullerene–DNA condensates did not change over 24 h for samples analyzed at several hour intervals.

When a smaller amount of **1** was used, we saw largely intact DNA rather than the disks: When a larger amount of **1** was added ($R = 2.6$), we found that the fullerene–DNA disks glued together to form a single-layer domain (Figure 3e). Double and triple layers were also found. When the fullerene–DNA mixture ($R = 2.6$) was washed with EtOH, we found an extremely small number of micrometer-sized aggregates with a mesh structure (Figure 3f). These objects are similar in size to the smallest phagocytes that we found inside the cells in the transfection experiments.[1]

The above experiments indicated that the fullerene **1** condenses plasmid DNA into compactly folded single-DNA disks, and then to multi-DNA objects as the amount of the

  1433-7851/01/4018-3365 $ 17.50+.50/0

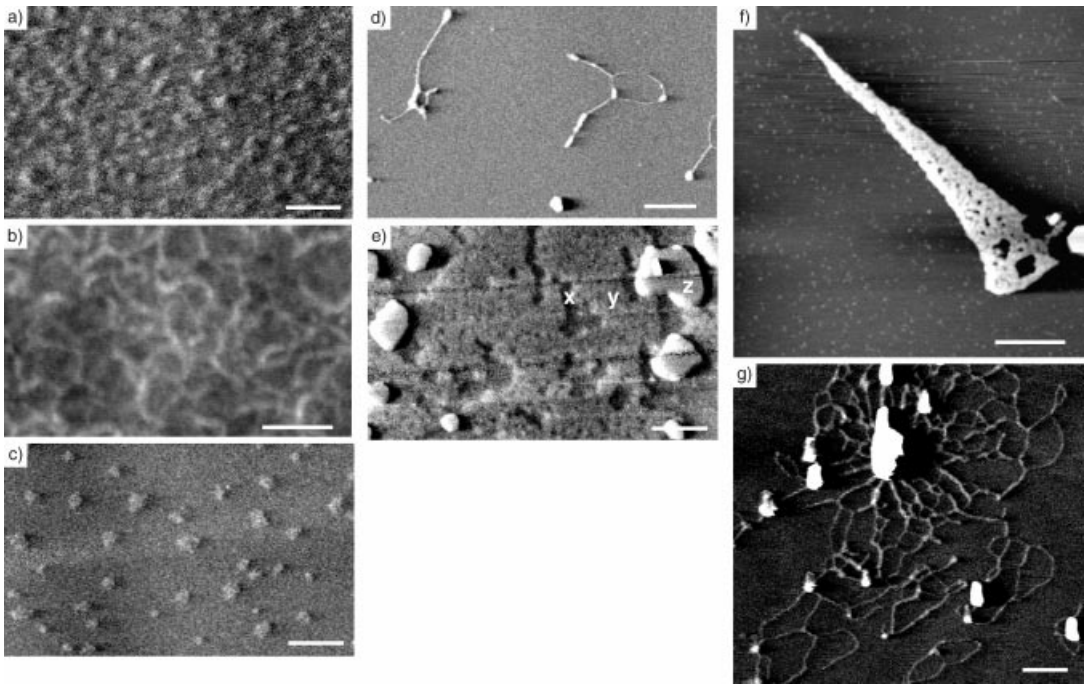

Figure 3. AFM images (micrometer-scale areas) of aggregates of fullerene **1** (a), and pBR322 DNA in the absence (b) and presence (c – g) of **1** at various R values. a) Vesicles of fullerene **1**; b) intact multiple DNA molecules, $R = 0$; c) disk-shaped DNA condensates, $R = 0.65$; d) partially condensed DNA molecules, $R = 0.65$; e) multiple fullerene – DNA condensates, $R = 2.6$ (bare mica surface is marked with x, a first layer of fullerene – DNA aggregates with y, and a second layer with z); f) an EtOH-precipitated giant aggregate; g) multiple DNA molecules after $CHCl_3$ extraction. All scale bars 200 nm. See Supporting Information for the detailed experimental procedure.

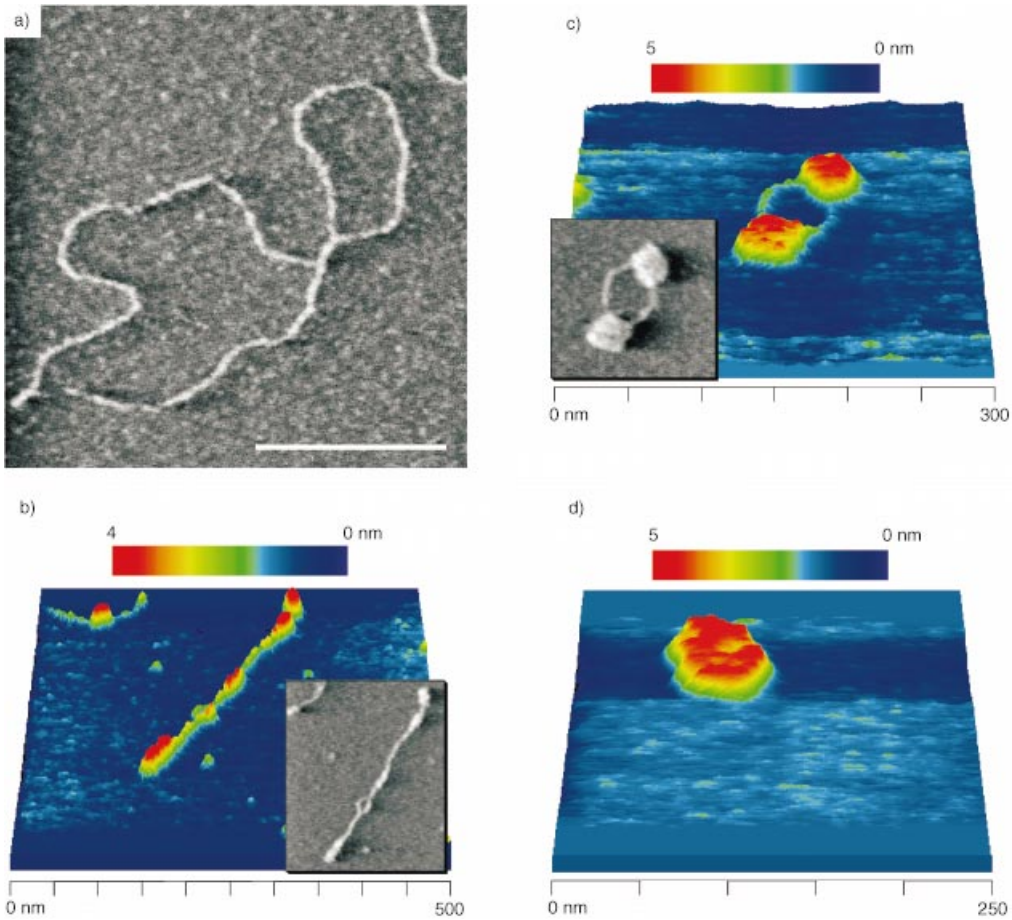

Figure 4. AFM images (submicrometer scale) of pBR322 DNA in the absence (a) and in the presence (b – d) of **1** at various R values. a) Intact DNA, $R = 0$; b) partially folded single DNA molecule, $R = 0.65$; c) partially condensed DNA with unfolded double strands, $R = 0.65$; d) fully condensed fullerene – DNA disk, $R = 0.65$. All scale bars 200 nm. Top views are given in black-and-white images. See Supporting Information for details of the experimental procedure.

  1433-7851/01/4018-3366 $ 17.50+.50/0

fullerene in solution increases. When the fullerene was removed from the solution, we could release DNA out of the condensate. Thus, when the fullerene in the $R = 2.6$ mixture was extracted with $CHCl_3$, AFM analysis of the aqueous phase (the same sample used for the gel analysis in Figure 1) largely showed individual DNA molecules together with a small number of large aggregates surrounded by numerous partially folded DNA molecules (Figure 3g). The image in Figure 3g resembles the classical picture of an *E. coli* nucleus from which histone protein was washed away after surfactant treatment.[7]

In summary, we have demonstrated that the fullerene **1** can fold a supercoiled DNA molecule into a single-molecule condensate through adhesion of DNA double strands. The rough estimate indicated that the fullerene folds the DNA with only a small increase of the volume of DNA. Such high efficiency of histone-like activity is remarkable since natural histone protein forms a chromatin structure with a volume increasing of ten to hundred times that of DNA.[8] The formation of disklike condensates composed of a single to a few DNA molecules is unique among the cases of other DNA-condensating agents based on lipid or dendrimers, which create much larger and less structurally defined DNA aggregates.[9] In the light of remarkably high tendency of water-soluble fullerene to form robust vesicles,[4] the process of fullerene–DNA condesation must involve collisions between a fullerene vesicle and a DNA molecule rather than a molecule–molecule interaction. The condensation process is largely kinetically controlled rather than thermodynamically controlled, as is known generally for polyelectrolyte–surfactant complexes.[10] We have found that the DNA condensation is dependent on the concentration of the DNA-binding fullerene. Translation of this observation into biology, we can speculate that in the cytoplasm the ester linkage in the fullerene **1** gradually yields to hydrolase activity,[11] which will detach the tetramino DNA binding sites from the fullerene core and hence results in the release of DNA from the aggregate. We are currently studying the structure activity relationship in the fullerene-mediated transfection.

Received: March 19, 2001 [Z16802]

[1] E. Nakamura, H. Isobe, N. Tomita, M. Sawamura, S. Jinno, H. Okayama, *Angew. Chem.* **2000**, *112*, 4424–4427; *Angew. Chem. Int. Ed.* **2000**, *39*, 4254–4257.

[2] a) H. Tokuyama, S. Yamago, E. Nakamura, T. Shiraki, Y. Sugiura, *J. Am. Chem. Soc.* **1993**, *115*, 7918–7919; b) E. Nakamura, H. Tokuyama, S. Yamago, T. Shiraki, Y. Sugiura, *Bull. Soc. Chem. Jpn.* **1996**, *69*, 2143–2151; c) S. Yamago, H. Tokuyama, E. Nakamura, K. Kikuchi, S. Kananishi, K. Sueki, H. Nakahara, S. Enomoto, F. Ambe, *Chem. Biol.* **1995**, *2*, 385–389; d) K. Irie, Y. Nakamura, H. Ohigashi, H. Tokuyama, S. Yamago, E. Nakamura, *Biosci. Biotechnol. Biochem.* **1996**, *60*, 1359–1361.

[3] H. G. Hansma, J. Vesenka, C. Siegerist, G. Kelderman, H. Morrett, R. L. Sinsheimer, V. Elings, C. Bustmante, P. K. Hansma, *Science* **1992**, *256*, 1180–1184.

[4] a) M. Sawamura, N. Nagahama, M. Toganoh, U. E. Hackler, H. Isobe, E. Nakamura, S.-Q. Zhou, B. Chu, *Chem. Lett.* **2000**, 1098–1099; b) S. Zhou, C. Burger, B. Chu, M. Sawamura, N. Nagahama, M. Toganoh, U. E. Hackler, H. Isobe, E. Nakamura, *Science* **2001**, *291*, 1944–1947; c) M. Matsumoto, H. Tachibana, R. Azumi, M. Tanaka, T. Nakamura, G. Yunome, M. Abe, S. Yamago, E. Nakamura, *Langmuir*, **1995**, *11*, 660–665.

[5] A. M. Cassell, W. A. Scrivens, J. M. Tour, *Angew. Chem.* **1998**, *110*, 1670–1672; *Angew. Chem. Int. Ed.* **1998**, *37*, 1528–1531.

[6] Heterogeneous distribution of various objects on the mica surface is likely due to the difference of the affinity of each object to the surface.

[7] R. Kavenoff, O. A. Ryder, *Chromosoma* **1976**, *55*, 13–25.

[8] B. Alberts, D. Bray, J. Lewis, M. Raff, K. Roberts, J. D. Watson, *Molecular Biology of the Cell*, 3rd ed., Garland, New York, NY, **1994**, pp. 335–399.

[9] a) L. A. Wangerek, H.-H. M. Dahl, T. J. Senden, J. B. Carlin, D. A. Jans, D. E. Dunstan, P. A. Ioannou, R. Williamson, S. M. Forrest, *J. Gene Med.* **2001**, *3*, 72–81; b) M. Laus, K. Sparnacci, B. Ensoli, S. Butto, A. Caputo, I. Mantovani, G. Zuccheri, B. Samori, L. Tondelli, *J. Biomater. Sci. Polym. Ed.* **2001**, *12*, 209–228; c) M. A. W. Eaton, T. S. Baker, C. F. Catterall, K. Crook, G. S. Macaulay, B. Mason, T. J. Norman, D. Parker, J. J. B. Perry, R. J. Taylor, A. Turner, A. N. Weir, *Angew. Chem.* **2000**, *112*, 4229–4233; *Angew. Chem. Int. Ed.* **2000**, *39*, 4063–4067; d) C. Kawaura, A. Noguchi, T. Furuno, M. Nakanishi, *FEBS Lett.* **1998**, *421*, 69–72; e) H. G. Hansma, R. Golan, W. Hsieh, C. P. Lollo, P. Mullen-Ley, D. Kwoh, *Nucleic Acids Res.* **1998**, *26*, 2481–2487; f) D. D. Dunlap, A. Maggi, M. R. Soria, L. Monaco, *Nucleic Acids Res.* **1997**, *25*, 3095–3101; g) V. J. Dzau, M. J. Mann, R. Morishita, Y. Kaneda, *Proc. Natl. Acad. Sci. USA* **1996**, *93*, 11421–11425.

[10] S. Zhou, C. Burger, F. Yeh, B. Chu, *Macromolecules* **1998**, *31*, 8157–8163.

[11] a) D. M. Lynn, R. Langer, *J. Am. Chem. Soc.* **2000**, *122*, 10761–10768; b) A. M. Aberle, F. Tablin, J. Shu, N. J. Walker, D. C. Gruenert, M. H. Nantz, *Biochemistry* **1998**, *37*, 6533–6540; c) J. Zhu, R. J. Munn, M. H. Nantz, *J. Am. Chem. Soc.* **2000**, *122*, 2645–2646; d) Y.-b. Lim, Y. H. Choi, J.-s. Park, *J. Am. Chem. Soc.* **1999**, *121*, 5633–5639.

Zero-Strain Intercalation Cathode for Rechargeable Li-Ion Cell

Jaephil Cho, Yong Jeong Kim, Tae-Joon Kim, and Byungwoo Park*

The market for Li-ion batteries is undergoing rapid expansion, as portable electronic devices demand a higher energy density and a better cycle life. Even though the $Li_{1-x}CoO_2$ cathode has been widely used in commercial Li-ion batteries, electrochemical charge (Li de-intercalation) and discharge (Li intercalation) produces a phase transition accompanying nonuniform strain, which is closely related to capacity fading.[1–3] This nonuniform dimensional change induces a shearing stress within each particle, and consequently fractures occur in most oxides.[2–4] Hence, a zero-strain cathode material, the lattice constants of which do not change during cycling, is ideal for a long operational lifetimes.[5–7] Here we report a zero-strain $LiCoO_2$ cathode material produced by thin-film coating of high-fracture-toughness

[*] Prof. Dr. B. Park, Y. J. Kim, T.-J. Kim
School of Materials Science and Engineering
Seoul National University
Seoul 151-744 (Korea)
Fax: (+82) 2-883-8197
E-mail: byungwoo@snu.ac.kr
Dr. J. Cho
Energy Laboratory
Samsung SDI Co., Ltd, Chonan, Chungchongnam-Do (Korea)

  1433-7851/01/4018-3367 $ 17.50+.50/0